OncoTargets and Therapy

Dovepress
open access to scientific and medical research

Open Access Full Text Article

ORIGINAL RESEARCH

Induction Of XLF And 53BP1 Expression Is Associated With Temozolomide Resistance In Glioblastoma Cells

This article was published in the following Dove Press journal:
OncoTargets and Therapy

Tongxia Zhang[1]
Jie Chai[2]
Lingyi Chi[3,4]

[1]Research Institute of Neuromuscular and Neurodegenerative Diseases and Department of Neurology, Qilu Hospital of Shandong University, Jinan 250012, People's Republic of China; [2]Department of Gastrointestinal Surgery, Shandong University Affiliated Shandong Cancer Hospital and Institute, Jinan, People's Republic of China; [3]Department of Neurosurgery, Qilu Hospital of Shandong University and Institute of Brain and Brain-Inspired Science, Shandong University, Jinan 250012, People's Republic of China; [4]Shandong Key Laboratory of Brain Function Remodeling, Jinan, Shandong 250012, People's Republic of China

Introduction: Glioblastoma (GBM) is the most commonly diagnosed primary brain tumor in adults. The 14.6 months median survival period of GBM patients is still palliative due to resistance to the first-line chemotherapeutic agent temozolomide (TMZ).

Methods: The cell growth inhibition effect was assessed using the SRB assay. The mRNA expression levels were examined using RT-qPCR. The protein expression levels were determined using Western blot analysis. The DNA repair by non-homologous end-joining (NHEJ) was quantified using NHEJ reporter assay. The TMZ-induced apoptosis was detected by the Caspase 3/7 activity kit. The DNA binding activity in cells was determined using chromatin fractionation assay. The 53BP1 inhibitor was identified using virtual screening followed by Western blot analysis. The synergy between TMZ and 53BP1 inhibitor in vivo was analyzed using a xenograft mouse model.

Results: We found that non-homologous end joining (NHEJ), which is one of the major DNA double-strand break repair pathways, participates in acquired TMZ-resistance in GBM. Canonical NHEJ key factors, XLF and 53BP1, are upregulated in TMZ-resistant GBM cells. Depletion of XLF or 53BP1 in TMZ-resistant cells significantly improve the potency of TMZ against GBM cell growth. Importantly, we identified a small molecule HSU2018 to inhibit 53BP1 at nanomolar concentration. The combination of HSU2018 and TMZ generates excellent synergy for cell growth inhibition in TMZ-resistant GBM cells and xenograft.

Conclusion: Our data suggest that NHEJ is a novel mechanism contributing to TMZ-resistance, and its key factors may serve as potential targets for improving chemotherapy in TMZ-resistant GBM.

Keywords: glioblastoma, temozolomide, XLF, 53BP1, non-homologous end joining, chemoresistance, 53BP1 inhibitor

Introduction

Glioblastoma (GBM) is a deadly, malignant brain tumor arising from glial cells.[1] Patients of GBM show high cellular heterogeneity and complex chromosome aberrations.[2,3] GBM is a severe brain tumor with a median survival time of only 12–15 months after the initial diagnosis.[4] The conventional therapies for newly diagnosed GBM patients are surgical resection followed by chemotherapy and radiation therapy. Temozolomide (TMZ), which is an alkylating agent, has been applied as the first-line chemotherapeutic regimen since 2005.[5] Although TMZ has been contributed to improve life quality and survival time of GBM patients, intrinsic and acquired resistance to TMZ are still the major obstacles for GBM treatment.[6,7]

Correspondence: Lingyi Chi
Department of Neurosurgery, Qilu Hospital of Shandong University and Institute of Brain and Brain-Inspired Science, Shandong University, 107 Wenhua Xi Road, Jinan, Shandong 250012, People's Republic of China
Tel +86 18560085730
Email chilingyi2019@163.com

submit your manuscript | www.dovepress.com
DovePress
http://doi.org/10.2147/OTT.S221025

TMZ elicits cytotoxicity during replication by methylation at O^6 and N^7 positions of guanine, and at N^3 position of adenine that results in DNA breaks, which eventually leads to cell apoptosis.[8] Elevated expression of O^6-methylguanine-DNA methyltransferase (MGMT), which directly removes methyl group from O^6-methylguanine, has been reported as the major reason for TMZ resistance. However, recent case studies of TMZ resistance reported that a series of TMZ-resistant GBM patients exhibited deficiency of MGMT activity.[9] Therefore, it is urgent to understand the TMZ-resistance mechanism independent of MGMT and develop alternative chemotherapy strategies against GBM.

DNA double-strand break (DSB), which is one of the most dangerous and toxic DNA lesions, are generated frequently in human cells.[10] Misrepair or unrepair of DSBs results in mutation, chromosomal aberration, carcinogenesis, and cell death.[11] To maintain genome stability when DSB occurred, cells developed two major DSB repair pathways: non-homologous recombination (NHEJ) and homologous recombination (HR).[12,13] HR is considered as the accurate DSB repair pathway since sister chromatid is incorporated as the template during gap filling. However, this template-dependent feature of HR limits this repair mechanism in the S and G2 phases of the cell cycle, where sister chromatids are available.[14,15] NHEJ, on the other hand, is approachable throughout the whole cell cycle and much more tolerant of different forms of broken DNA ends.[16–20]

Here, we characterize the role of NHEJ key factor XLF and 53BP1 in TMZ-resistant GBM. Both mRNA level and protein level of these two factors are upregulated in TMZ-resistant LN18 and U87 cell lines. Importantly, XLF or 53BP1 deficiency re-sensitizes GBM cells to TMZ by 2–4 folds. We also demonstrated that TMZ treatment induces XLF and 53BP1 expression in TMZ-sensitive GBM cells. Importantly, we identified a potent 53BP1 inhibitor HSU2018 that degrades 53BP1 at 0.5 μM. HSU2018 exhibits excellent synergy with TMZ against GBM in vitro and in vivo. Our results suggest that XLF and 53BP are promising targets to overcome TMZ-resistance in GBM.

Methods And Materials

Cell Lines And Reagents

LN18 (ATCC, CRL-2610) and U87 cells (ATCC, HTB-14) were cultured at 37°C in 5% CO_2 atmosphere in DMEM and EMEM with 10% fetal bovine serum (FBS) for less than 6 months, respectively. Resistant cells were generated according to previous studies.[22] Briefly, LN18-TR and U87-TR cells were obtained by treating their parental cells with 200 μM TMZ for 6 hrs and released in drug-free media for 2 weeks. TMZ concentration was increased every 2 weeks up to 1 mM. TMZ (Sigma, T2577) was dissolved in DMSO and diluted in certain media.

Cell Viability Assay

GBM cells were seed at 4×10^3 cells/well and cultured for overnight. Cells were incubated with TMZ for 72 hrs and the cell viability was detected by using Sulforhodamine B (SRB) assay.[23] Cells were fixed by 100 μL/well of 10% trichloroacetic acid at 4°C for 1 hr. Plate was washed 4 times with slow running tap water and air-dried for 1 hr at room temperature (RT) or 20 mins in fume hood. Cells were stained by 100 μL/well 0.02% SRB in 1% acetate acid for 1 hr at RT. Plates were washed for 3 times with 200 μL/well 1% acetate acid and air dried. 200 μL/well of 10 mM Tris-HCl, pH 10.5 was added in each well to extract SRB with 1 hr shaking on an orbital shaker. The absorbance was measured at 510 nm by microplate reader (BioTek).

Quantitative Reverse Transcription-Polymerase Chain Reaction

Total RNA was isolated using the PureLink RNA Mini Kit (Invitrogen #12183018A). Complementary DNA was synthesized using the iScript™ cDNA Synthesis Kit (Bio-Rad #1708891) according to the manufacturer's instructions. Fluorescence real-time RT-PCR was performed with SsoAdvanced™ Universal SYBR® Green Supermix following the instruction manual (Bio-Rad #172-5274) and detected by CFX96 Dx System (Bio-Rad #1708891). The experiment was performed in triplicate and repeated at least three times.

Primers: Ku80 (Left: cgacaggtgtttgctgagaa, Right: tcacatccatgctcacgatt), DNA-PKcs (Left: tctgaaggggttgtcctcac, Right: tgggcacaccactttaacaa), Ligase IV (Left: agcctgacctggagaacaga, Right: catgcaggcttgacaacatc), XLF (Left: tctctggcctccccttctat, Right: gatctcgaatcagcgtagcc), XRCC4 (Left: cattgttgtcaggagcagga, Right: tctgcaggtgctcatttttg), MRE11 (Left: gccttcccgaaatgtcacta, Right: ttcaaaatcaacccctttcg), 53BP1 (Left: tgacagcacagcccagtaag, Right: cctcaggctctggtgacttc), RAD51 (Left: ctcagcctcccgagtagttg, Right: catcactgccagagagacca), RPA32 (Left: ccagtgggttgacacagatg, Right: tgataggtgctctccctgct), BRAC1 (Left: ctcaaggaaccagggatgaa, Right: gctgtaatgagctggcatga), EXO1 (Left: gctgtcagaagatgacctgttg, Right: gcac

cactttcttcatttttcc), Polδ (POLD3) (Left: agaaagccatgctaaaggacag, Right: catgtgaagatgtgactgctca), GAPDH (intrinsic control) (Left: cgagatccctccaaaatcaa, Right: ggtgctaagcagttggtggt)

Western Blot Analysis

Method has been described in previous works.[24] Briefly, protein samples were resuspended in SDS-PAGE sample buffer, and boiled for 5 mins at 95°C. The samples were loaded and separated on an 12% polyacrylamide gel (29:1) at 120 V for 1.5 hr on the electrophoresis apparatus (BioRad). Separated samples were transferred to nitrocellulose membrane at 100 V and 4°C in cold room for 45 mins. Membrane was blocked by 3% BSA diluted in PBS with 0.1% Tween 20 and probed by relevant antibody followed by HRP-conjugated rabbit secondary antibody. The protein signal was developed by SuperSignal™ west Femto Maximum Sensitivity Substrate (ThermoFisher Scientific #34096) and detected by ChemiDoc™ (BioRad). Antibodies: anti-XLF: abcam #33499; anti-53BP1: abcam #21083; anti-actin: abcam #8227.

NHEJ Reporter Assay

NHEJ reporter assay was previously described.[25] Briefly, 40 μg of NHEJ reporter plasmid were linearized by NheI in 50 μL for 6 hrs at 37°C. Linearized DNA was then extracted by using Qiagen gel extraction kit (Qiagen #28704). 2 μg of linearized DNA was transfected into LN18 or U87 cells by using Lipofectamine 3000 as previously described.[26] Cells with chromosomally integrated reporter constructs were selected by incubating in media with 1 mg/mL geneticin 24h after transfection for 2 weeks. Plasmid-integrated cells were seeded at 3×10^5 cells/mL in a 6-well plate and cultured for 24 hrs to allow adhere. 2μg/well of I-SceI was transfected into the cell by lipofectamine 3000 to recognize I-SceI site located in reporter plasmid and generate DSB. Cells were then incubated for 48 hrs to allow DSB repair by NHEJ. Repaired cells, which express GPF, were harvested by using trypsin and resuspend in PBS followed by quantification using flow cytometry (Beckman Coulter) to indicate NHEJ efficiency.

Chromatin Fractionation Assay

1×10^7 cells were harvested and washed twice in ice-cold PBS, and extracted twice in CSK buffer (100 mM NaCl, 300 mM sucrose, 3 mM $MgCl_2$, 0.7% Triton X-100, 10 mM PIPES, pH 7.0) supplemented with 1× protease inhibitor cocktail (Roche, 4693159001) and 0.4 mg/mL RNase A (Thermo Fisher, 12091021) at 4°C for 10 mins. Cells were then washed 3 times in ice-cold PBS and harvested in 2× SDS loading buffer for analysis by SDS-PAGE and Western blotting assay.

Transfection

For siRNA transfection, 50 nM of siXLF or si53BP1 was transfected in GBM cells by using Lipofectamine RNAiMAX (ThermoFisher) according to the manufacturer's instruction. SiGL2 was used as a negative control. Cell viability assay or reporter assay was performed 48 hrs after siRNA transfection. si53BP1-UTR: AAAUGUGUCUUGUGUGUAA (Sigma). siXLF-UTR (Dharmacon #A-014446-16-0005). siGL2 (intrinsic control): CGUACGCGGAAUACUUCGAUU (Sigma).

For ectopic expression, XLF and 53BP1 (Addgene #52507) plasmids were transfected in GBM cells by using Lipofectamine 3000 (ThermoFisher) 24 hrs after siRNA transfection. cDNA for XLF were cloned into pcDNA3 carrying a FLAG epitope (Invitrogen) using standard DNA cloning methods.

Caspase-3/7 Activity Assay

Caspase-3/7 activity was examined using SensoLyte® Homogeneous AMC Caspase-3/7 Assay kit (AnaSpec Inc., no. 7118) in LN18-TR and U87-TR cells according to the manufacturer's instructions.

Drug Screening

Virtual screening was performed by docking small molecule structure (ZINK database) to the available crystal structure of XLF (PDB: 2R9A) and 53BP1 (PDB: 1GZH and 2IG0) with Glide software 2.5 (Schrödinger, Inc, USA). The hydrogen bond acceptor, donor, hydrophobic and ring aromatic were adopted for calculations of all chemical feature. Estimated binding energy was used to rank inhibitor candidates. The small molecule with lowest binding energy was then further modified to achieve higher docking score. Top candidates were analyzed by using Western blotting assay for protein inhibition activity.

LN18-TR Xenograft

Thirty-two female BALB/c nude mice (5–6 weeks old, body weight 18–22 g) were randomly assigned to four groups, 8 mice per group. Note that 5×10^6 LN18-TR cells were injected subcutaneously into mice. Mice were treated intraperitoneally with control (DMSO), TMZ (20 mg/kg/3 day), HSU2018 (2mg/kg/3 days) and Combo (20 mg/kg/3 day of TMZ + 2 mg/kg/3 day of HSU2018) for 2 weeks. The tumor volume was

measured starting from day 10 after injection at a frequency of three times a week. Tumor volume, expressed in mm^3, was calculated using the following formula, V= (length × $width^2$)/2. Experiments were approved by Shandong University.

Statistical Analysis

Data are presented as the mean±SD of three independent experiments. Statistical evaluation was performed using the Student's *t*-test or one-way ANOVA. Differences were considered to be statistically significant when $P<0.05$. All statistical analyses were performed using Prism7 software (GraphPad Software, La Jolla, CA, USA).

Results

XLF And 53BP1 Are Upregulated In TMZ-Resistant Cells

To investigate the mechanism of TMZ-resistance in GBM, we first generated two TMZ-resistant GBM cell lines by incubating the LN18-wild type (LN18-WT) and U87-wild type (U87-WT) cells with TMZ for 4 months. As shown in Figure 1A and B, LN18-TMZ-resistant (LN18-TR) and U87-TMZ-resistant (U87-TR) cell line showed 4.47-fold and 4.76-fold increase of IC50, respectively, as compared to their parental cell lines.

To determine whether DSB pathways participate in TMZ-resistance, we used qPCT to examine the mRNA expression of canonical factors that are required for NHEJ and HR. Among NHEJ factors, including Ku80, DNA-PKcs, Ligase IV, XRCC4, XLF, MRE11 and 53BP1, XLF and 53BP1 were upregulated in LN18-TR cells by 4.5 and 3.1 folds, respectively (Figure 1C). To further confirm the upregulation of XLF and 53BP1 are consistent in GBM cell lines, we evaluated the mRNA levels of these factors in U87 cell lines. The mRNA expression levels of XLF and 53BP1 in U87-TR cells were about 4.2- and 2.5-fold higher than in U87-WT cells, respectively (Figure 1D). XLF is essential for NHEJ efficiency, therefore, our data suggest NHEJ pathway contributes to TMZ-resistance. Interestingly, 53BP1 participates in pathways choice between NHEJ and HR. Since the expression of 53BP1 was upregulated in TMZ-resistant cells, we next examined the mRNA expression levels of HR factors, including RAD51, RPA32, BRAC1, EXO1, and Polδ, in LN18 and U87 cell lines. As shown in Figure 1E and F, mRNA expression of HR key factors did not show a significant difference between TR and WT cells. These data indicate that NHEJ pathway participates in the TMZ-resistance mechanism.

TMZ Induces XLF And 53BP1 Expression In TMZ-Sensitive Cells

To further examine protein expression levels of XLF and 53BP1, we extracted whole cell lysate and compared the protein expression levels between TMZ sensitive and resistant cell lines. Using Western Blotting assay, we found that protein expression of both XLF and 53BP1 indeed increased in TMZ-resistant cells (Figure 2A and B; Supplementary Figure 1A and B). These data are consistent with the mRNA results as shown in Figure 1C and D. Since TMZ-resistant GBM cells were generated by incubating WT cells with TMZ, we hypothesize that the upregulation of XLF and 53BP1 in the TR cells result from response to TMZ treatment. To test our hypothesis, we incubated the TMZ-sensitive cells with different concentrations of TMZ for 48 hrs and evaluated protein expression levels of XLF and 53BP1. As shown in Figure 2C and D, XLF and 53BP1 expressions were increased in both LN18-WT and U87-WT cells treated with TMZ in a dose-dependent manner (Supplementary Figure 1C and D). Upregulated mRNA levels of XLF and 53BP1 in response to TMZ treatment were furthermore confirmed using qPCR (Figure 2E–H). These results suggest that XLF and 53BP1 may contribute to TMZ resistance in GBM cells.

XLF Or 53BP1 Depletion Improves TMZ Sensitivity In GBM Cells

Given that XLF and 53BP1 are upregulated at both translational and transcriptional levels in TMZ-resistant cells, it is encouraging to investigate whether XLF or 53BP1 deficiency re-sensitize TR cells to TMZ. We used siRNA to knockdown XLF or 53BP1 in LN18-TR cells and evaluated cell viability against TMZ. Significantly, XLF and 53BP1 depletion-sensitized LN18-TR cells to TMZ by 4.2 and 2.3 folds, respectively (Figure 3A). In support to this result, compromised XLF and 53BP1 expression also contributed to sensitize U87-TR cells to TMZ by 2.8 and 2 folds, respectively (Figure 3B). To exclude the possibility that the increased sensitivity to TMZ could be masked by siRNA off target effect, we complemented XLF and 53BP1 into XLF and 53BP1 knockdown cells, respectively. Since the siRNAs of XLF and 53BP1 target 5′UTR region of the genes, ectopic expression of these proteins was not affected (Supplementary Figure 2A and B). We found that

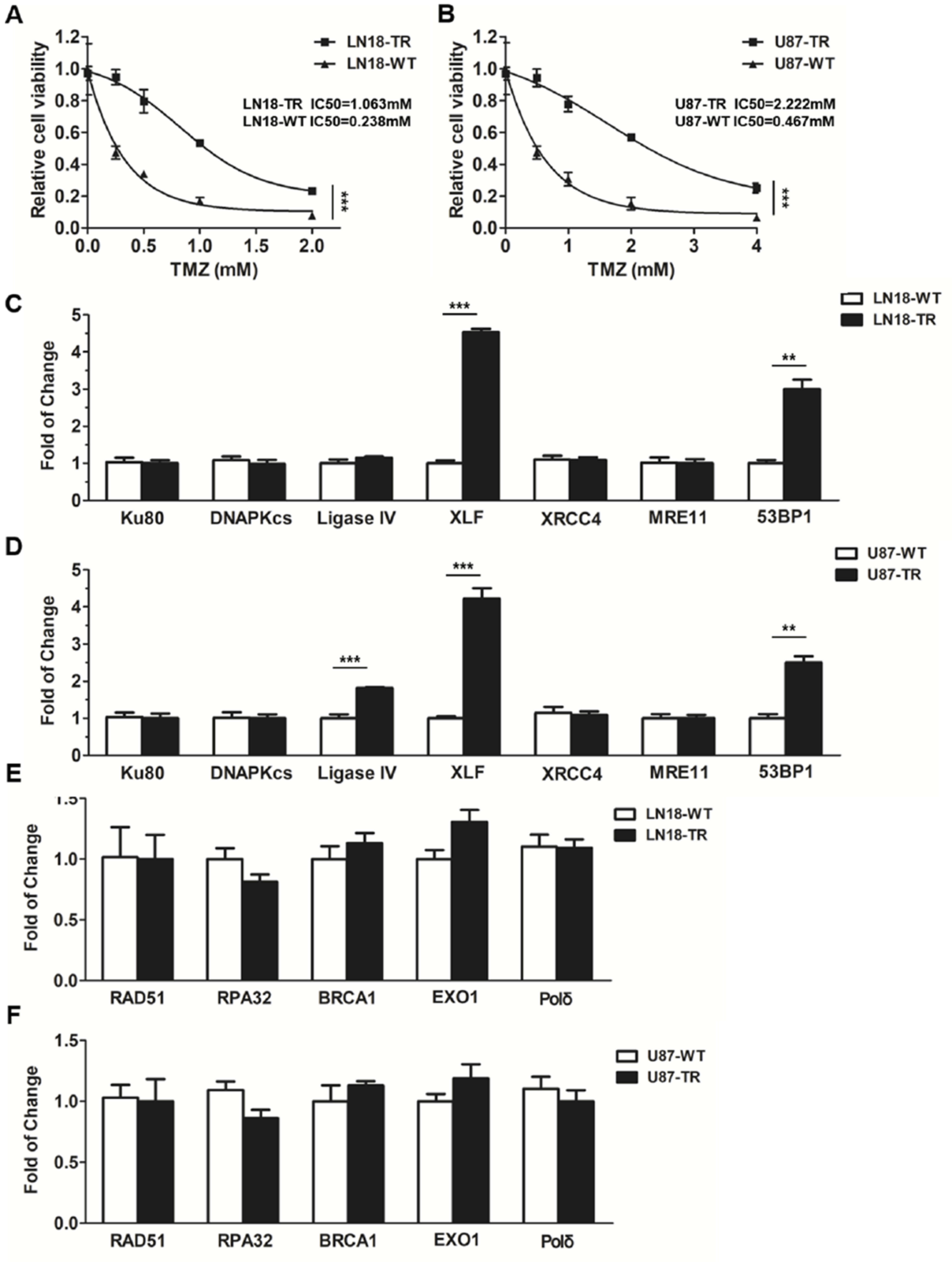

Figure 1 XLF and 53BP1 are upregulated in TMZ-resistant cells. (**A**) Cell viability of TMZ-sensitive and TMZ-resistant LN18 cell line. TMZ concentrations are 0 mM, 0.25 mM, 0.5 mM, 1 mM and 2 mM. LN18-TR: LN18-TMZ-resistant cell line. (**B**) Cell viability of TMZ-sensitive and TMZ-resistant U87 cell line. TMZ concentrations are 0 mM, 0.5 mM, 1 mM, 2 mM and 4 mM. U87-TR: U87-TMZ-resistant cell line. (**C**) mRNA expression of Ku80, DNAPKcs, ligase IV, XLF, XRCC4, MRE11 and 53BP1 in LN18 cell lines. (**D**) mRNA expression of Ku80, DNAPKcs, ligase IV, XLF, XRCC4, MRE11 and 53BP1 in U87 cell lines. (**E**) mRNA expression of RAD511, RPA32, BRCA1, EXO1, and Pol δ in LN18 cell lines. (**F**) mRNA expression of RAD511, RPA32, BRCA1, EXO1, and Pol δ in U87 cell lines. **p<0.01, ***p<0.001.

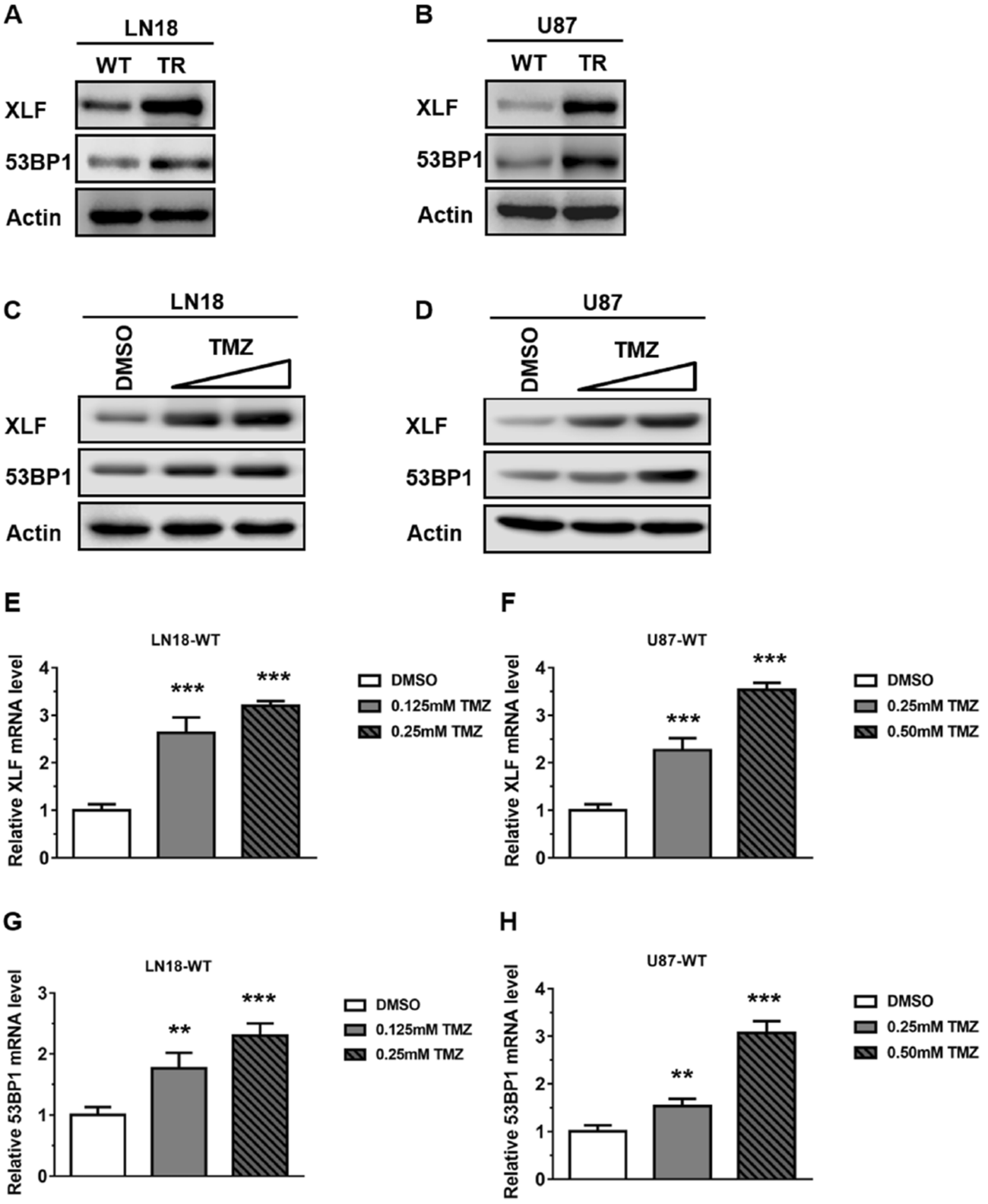

Figure 2 TMZ induces XLF and 53BP1 expression in TMZ-sensitive cells. (**A**) Immunoblotting of XLF and 53BP1 protein expression in LN18 cell lines. (**B**) Immunoblotting of XLF and 53BP1 protein expression in U87 cell lines. (**C**) Immunoblotting of XLF and 53BP1 protein expression in LN18-WT treated with TMZ. LN18-WT was treated with 0.125 mM and 0.25 mM of TMZ. (**D**) Immunoblotting of XLF and 53BP1 protein expression in U87-WT treated with TMZ. U87-WT was treated with 0.25 mM and 0.5 mM of TMZ. (**E**) Gene expression levels of XLF were determined by qRT-PCR in TMZ treated LN18-WT cells. (**F**) Gene expression levels of XLF were determined by qRT-PCR in TMZ treated U87-WT cells. (**G**) Gene expression levels of 53BP1 were determined by qRT-PCR in TMZ treated LN18-WT cells. (**H**) Gene expression levels of 53BP1 were determined by qRT-PCR in TMZ treated U87-WT cells. Results represent the mean ± SD of three independent experiments. **P<0.01, ***P<0.001.

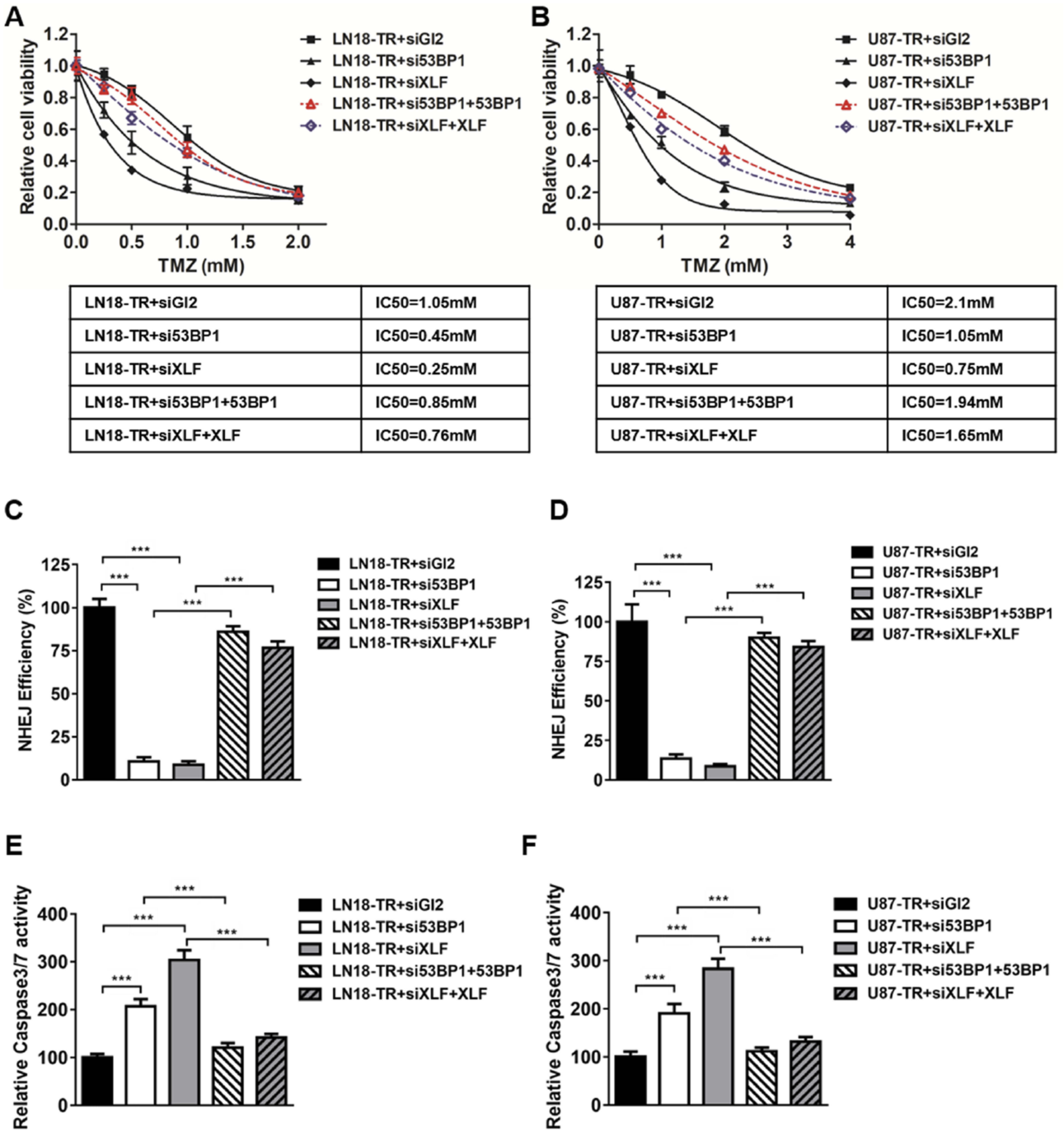

LN18-TR+siGl2	IC50=1.05mM
LN18-TR+si53BP1	IC50=0.45mM
LN18-TR+siXLF	IC50=0.25mM
LN18-TR+si53BP1+53BP1	IC50=0.85mM
LN18-TR+siXLF+XLF	IC50=0.76mM

U87-TR+siGl2	IC50=2.1mM
U87-TR+si53BP1	IC50=1.05mM
U87-TR+siXLF	IC50=0.75mM
U87-TR+si53BP1+53BP1	IC50=1.94mM
U87-TR+siXLF+XLF	IC50=1.65mM

Figure 3 XLF or 53BP1 depletion improves TMZ sensitivity in GBM cells. (**A**) Cell viability in LN18-TR+siGL2, LN18-TR+si53BP1, LN18-TR+siXLF, LN18-TR+si53BP1 with 53BP1 ectopic expressed and LN18-TR+siXLF with XLF ectopic expressed cell lines. TMZ concentrations are 0 mM, 0.25 mM, 0.5 mM, 1 mM and 2 mM. IC_{50}s of TMZ was indicated. (**B**) Cell viability in U87-TR+siGL2, U87-TR+si53BP1, U87-TR+siXLF, U87-TR+si53BP1 with 53BP1 ectopic expressed and U87-TR+siXLF with XLF ectopic expressed cell lines. TMZ concentrations are 0 mM, 0.5 mM, 1 mM, 2 mM and 4 mM. IC_{50}s of TMZ was indicated. (**C**) NHEJ efficiency in LN18-TR+siGL2, LN18-TR +si53BP1, LN18-TR+siXLF, LN18-TR+si53BP1 with 53BP1 ectopic expressed and LN18-TR+siXLF with XLF ectopic expressed cell lines. NHEJ efficiency of LN18-TR +siGL2 is normalized to 100%. (**D**) NHEJ efficiency in U87-TR+siGL2, U87-TR+si53BP1, U87-TR+siXLF, U87-TR+si53BP1 with 53BP1 ectopic expressed and U87-TR +siXLF with XLF ectopic expressed cell lines. NHEJ efficiency of U87-TR+siGL2 is normalized to 100%. (**E**) Caspase-3/7 activity in LN18-TR and (**F**) U87-TR cells was assessed using the SensoLyte Homogeneous AMC Caspase-3/7 assay kit. Results represent the mean ± SD of three independent experiments. ***P<0.001.

TMZ resistance can be successfully rescued by ectopic expression of 53BP1 and XLF (Figure 3A and B).

To determine whether the improved sensitivity to TMZ, which was generated by XLF or 53BP1 in TR cells, is mediated by NHEJ efficiency, we incorporated NHEJ reporter assay to measure NHEJ efficiency in XLF or 53BP1 deficient cells. We first knocked down XLF or 53BP1 in LN18-TR and U87-TR cells, which was stably transfected

with NHEJ reporter. DSBs were then introduced by using I-SceI restriction enzyme and cells were incubated for another 48 hrs to allow DSB repair by NHEJ. Repaired cells express GPF that can be quantified by flow cytometry to indicate NHEJ efficiency. As shown in Figure 3C and D, both 53BP1 and XLF deficiency led to significant decrease of NHEJ efficiency in TMZ-resistant cells. Interestingly, NHEJ efficiency is elevated in TMZ-resistant cells as compared to their parental cells, indicating that inhibition of XLF or 53BP1 sensitizes GBM cells to TMZ via compromising NHEJ efficiency (Supplementary Figure 3A and B). To the end of investigating the mechanism by which XLF and 53BP1 deficiency increase cell growth inhibition, we found that caspase3/7 activity was profoundly promoted in cells lack of XLF or 53BP1 (Figure 3E and F). These results indicate that inhibition of NHEJ by depleting XLF or 53BP1 sensitzes GBM cells to TMZ via promoting apoptosis.

TMZ Induces DNA Binding Activity Of XLF And 53BP1 In GBM Cells

Although XLF does not have enzymatic activity, it facilitates NHEJ through tethering DNA breaks.[21] In addition, 53BP1 is also a well-established DNA binding protein. Therefore, we investigated whether XLF- or 53BP1-DNA interaction is affected by TMZ treatment. We used the chromatin fractionation assay to examine their DNA binding activities after acute treatment in LN18-WT cells with 5 mM TMZ for 2 hrs. As shown in Figure 4A and Supplementary Figure 4A, chromatin-bound XLF and 53BP1 were significantly increased

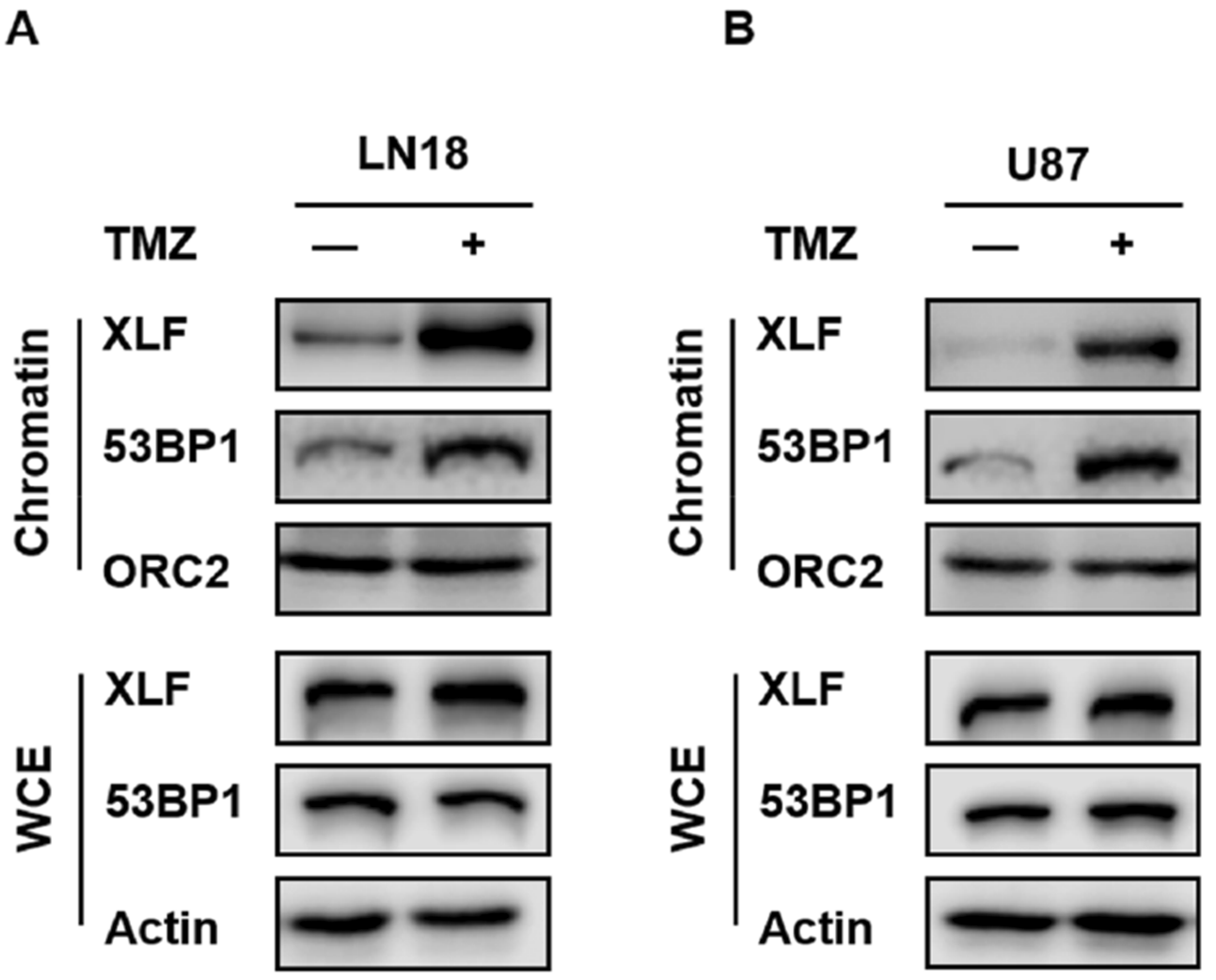

Figure 4 TMZ induces DNA binding activity of XLF and 53BP1 in GBM cells. (**A**) Chromatin fractionation of XLF and 53BP1 in LN18-WT treated with TMZ. LN18-WT was treated with 5 mM of TMZ for 2 hrs. WCE: whole-cell extract. (**B**) Chromatin fractionation of XLF and 53BP1 in U87-WT treated with TMZ. U87-WT was treated with 10 mM of TMZ for 2 hrs. WCE: whole-cell extract.

after TMZ treatment while the total levels of these proteins were not affected within 2 hrs. We also observed the similar results using U87-WT cells (Figure 4B; Supplementary Figure 4B). Our data suggest TMZ induces DNA binding activity of both XLF and 53BP1, and increased NHEJ efficiency in TMZ resistance cells may be due to more efficient interaction between DNA and NHEJ factors.

53BP1 Inhibitor Re-Sensitizes GBM Cells To TMZ

Given that both XLF and 53BP1 contribute to TMZ resistance in GBM, our group was interested in developing XLF and 53BP1 inhibitors. In a screening to identify small molecules that target XLF or 53BP1, we found that HSU2018 (Figure 5A) interacts with 53BP1 and markedly degrades 53BP1 in both LN18-TR and U87-TR cells by using Western blotting assay (Figure 5B and C; Supplementary Figure 5A and B). Significantly, HSU2018 generated 53BP1 degradation at 0.5 μM in both TMZ-resistant cell lines, indicating that HSU2018 is a very potent 53BP1 inhibitor. Since 53BP1 is one of the key factors of NHEJ regulation, we then evaluated NHEJ efficiency in the presence of HSU2018. As we expected, as a 53BP1 inhibitor, HSU2018 impaired NHEJ efficiency in a dose-dependent fashion in TMZ-resistant GBM cells (Figure 5D and E). To determine whether HSU2018 can improve TMZ sensitivity in GBM cells, we treated TMZ-resistant cells with 0.5 μM HSU2018 for 48 hrs and combined with 0 to 2 mM of TMZ for another 72 hrs. By using cell viability assay, we found that HSU2018 decreased IC_{50} of TMZ by 3.6 and 2.7 folds in LN18-TR and U87-TR cells, respectively (Figure 5F and G). Importantly, 0.5 μM of HSU2018 did not result in severe cell death, indicating that HSU2018 is a promising TMZ sensitizer with low toxicity at an effective dose.

To further evaluate the potency of HSU2018 in combine with TMZ in vivo, we subcutaneously implanted LN18-TR cells into 5–6 weeks old female nude mice to form TMZ-resistant GBM tumors. The mice were then treated with control (DMSO), HSU2018, TMZ or combination of both via intraperitoneal injection. We found that, similar to the result of in vitro cell survival assay, the combinational chemotherapy with TMZ and HSU2018 exhibited an excellent synergy in reducing tumor growth as compared to TMZ or HSU2018 treatment alone (Figure 6A–C). Together our results suggest that inhibition of 53BP1 is a promising therapeutic approach to overcome TMZ-resistance in GBM.

Discussion

In this study, we identified two NHEJ factors that contribute to acquired TMZ-resistant GBM. Depletion of XLF or 53BP1 significantly improved therapeutic effect of TMZ, suggesting a role of NHEJ pathway in chemoresistance in GBM. Importantly, we identified a very potent 53BP1 inhibitor HSU2018 that inhibits 53BP1 protein expression. This small molecule generates great synergy with TMZ at 0.5 μM in reducing cell survival and tumor growth.

DNA has been targeted in various types of cancers to generate DNA lesions that eventually lead to cell death since 1940s.[27] However, efficient DNA repair could impede the therapeutic effect and contribute to chemoresistance. Therefore, determine whether certain DNA repair pathway participates in TMZ-resistance may provide promising ways to overcome the recurrence of GBM after chemotherapy. Although mismatch repair and upregulated MGMT are most studied TMZ-resistance mechanism, emerging evidences indicate that DSB repair pathways may also prevent cell death in GBM.[28,29] NHEJ is the predominant DSB repair pathway in human that can be used in the whole cell cycle. Importantly, NHEJ repairs most of the DSBs generated by ionizing radiation. Therefore, inhibition of NHEJ may sensitize glioma cells to radiotherapy, which is commonly used for GBM treatment, to overcome radioresistance.

The DSB ends constructions are important for the pathway choice between HR and NHEJ. HR requires DNA end resection to initiate the repair, while NHEJ is inhibited when the gap of two broken ends reaches 3–4 nucleotides.[30] Therefore, 53BP1, which prevents DNA end resection, is considered to facilitate the transition from HR to NHEJ.[31] NHEJ is initiated with the interaction between Ku70/80 heterodimer and DSB in a sequence-independent manner.[32] Once Ku-DNA complex formed, Ku recruits other NHEJ required factors including DNA-dependent protein kinase catalytic subunit (DNA-PKcs), the X-ray repair cross-complementing 4 (XRCC4)-ligase IV complex and the XRCC4-like factor protein (XLF, also as known as Cernunnos).[33–35] Although NHEJ is well recognized, the mechanism of how NHEJ factors assemble is not thoroughly studied. One of the theories of NHEJ assembly demonstrates that XLF and XRCC4 form long filaments wrapping around broken DNA ends to promote ends approximation.[21,36] XLF is a relative new NHEJ key factor discovered by two laboratories in 2006.[37,38] XLF functions as homodimer and facilitates ligation in NHEJ.[39]

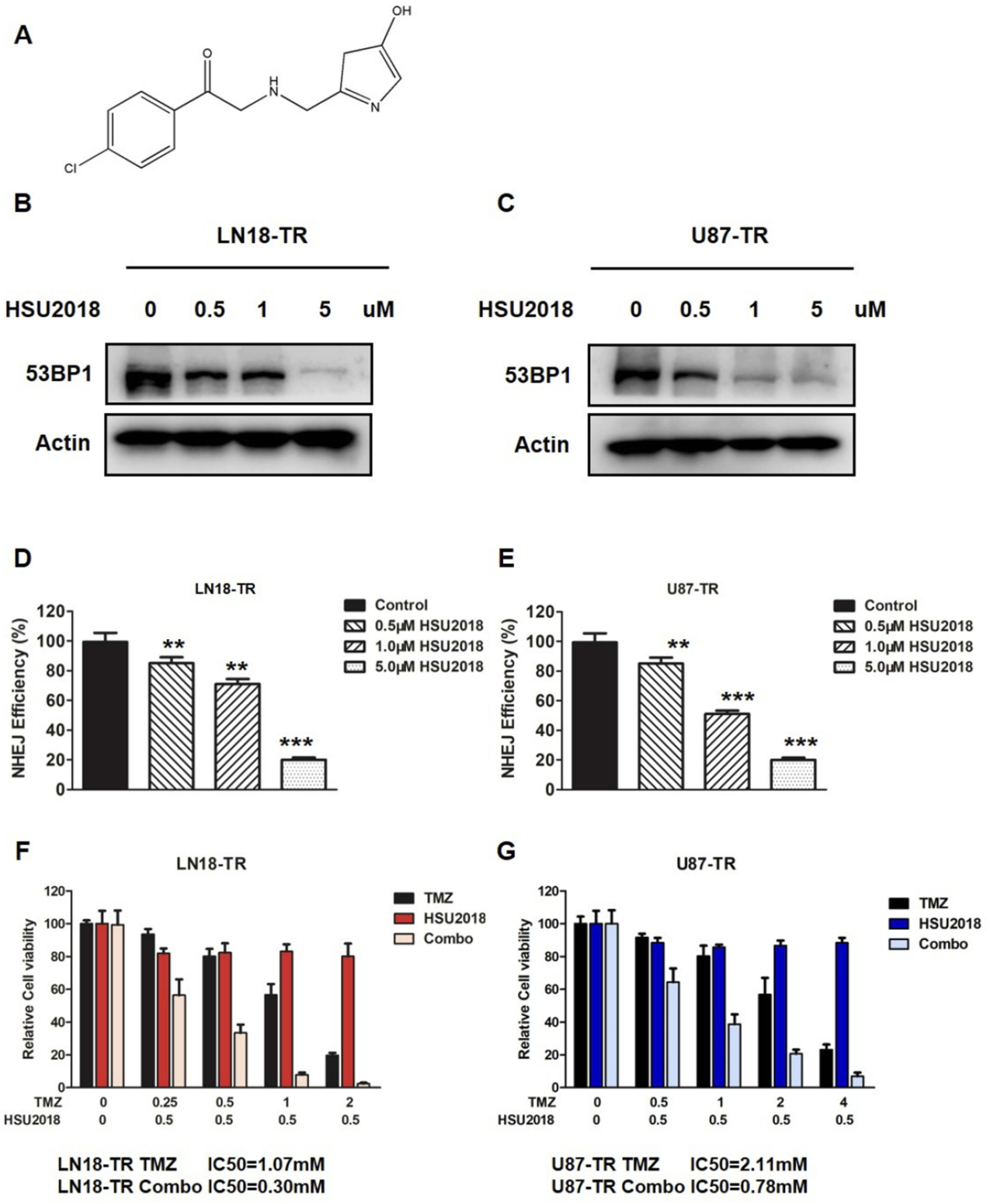

Figure 5 53BP1 inhibitor re-sensitizes GBM cells to TMZ. (**A**) The chemical structure of HSU2018. (**B**) LN18-TR and (**C**) U87-TR cells were treated with HSU2018 for 48 hrs. 53BP1 protein expression was analyzed by using Western blotting assay against the anti-53BP1 antibody. (**D**) NHEJ efficiency in LN18-TR and (**E**) U87-TR cells treated with HSU2018. HSU2018 was added to the cells 48 hrs before I-SceI transfection. **P<0.01, ***P<0.001. (**F**) HSU2018 sensitizes TMZ-resistant LN18 and (**G**) U87 cells to TMZ. 0.5 μM HSU was added to TR cells 48 hrs before TMZ treatment.

However, enzymatic activity of XLF has not been found. XLF may serve as scaffold protein by interacting with XRCC4 to tether DNA ends. It is interesting to observe that TMZ-induced chromatin binding of XLF and 53BP1.

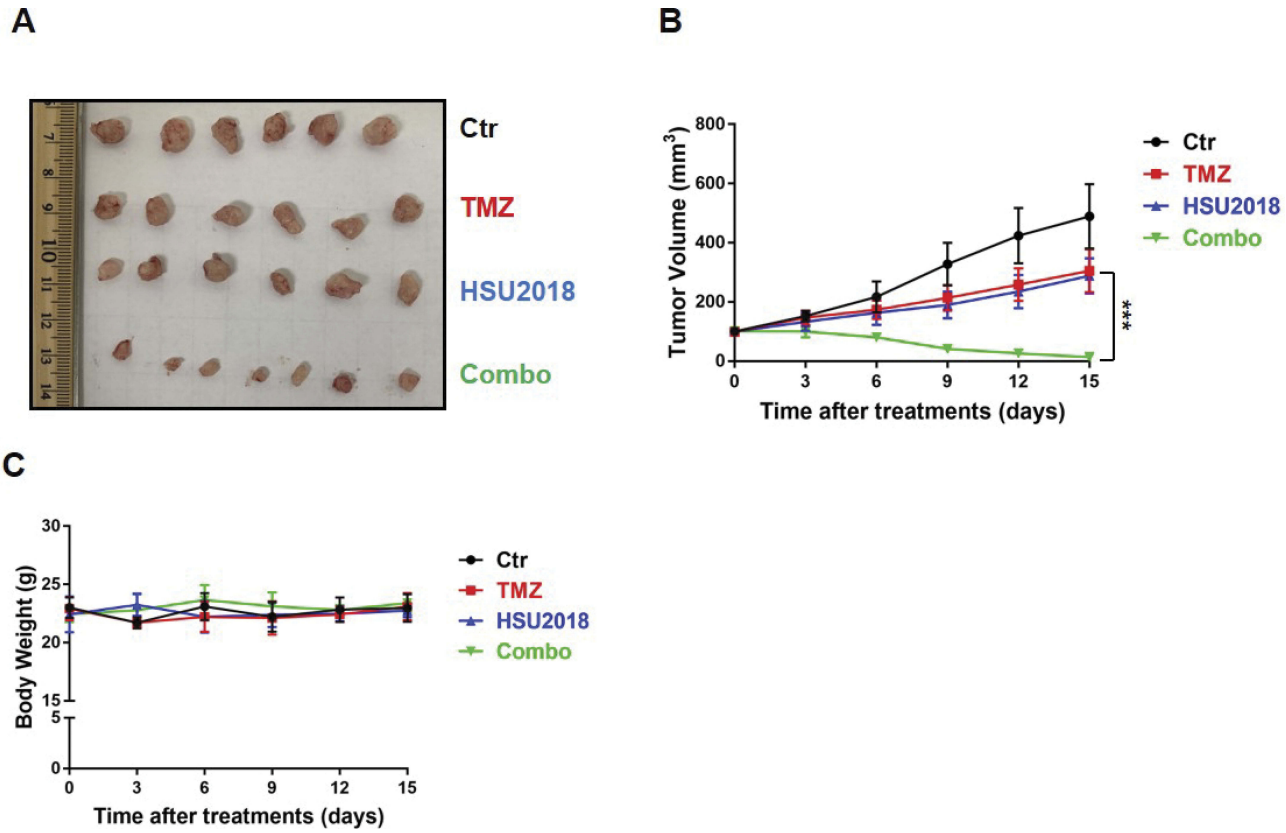

Figure 6 HSU2018 restores sensitivity to TMZ in LN18-TR xenograft model. (**A**) Representative images of xenograft tumor. LN18-TR xenograft mice treated with control (DMSO), TMZ (20 mg/kg/3day intraperitoneally), HSU2018 (2 mg/kg/3days), and Combo (20 mg/kg/3day of TMZ +2 mg/kg/3day of HSU2018). (**B**) Tumor volume was reported in mm^3 as the mean ± SD and statistically compared between TMZ and Combo tumors. n ≥6 tumors/group. ***P < 0.001. (**C**) Body weight was measured twice a week as the mean ± SD. n ≥6 tumors/group.

Given that NHEJ efficiency is elevated in TMZ-resistant cells, acquired TMZ-resistance may result from improved NHEJ achieved by more efficient DNA binding and tethering.

Since the alternative chemotherapies of GBM are very limited, identification of new targets to improve sensitivity to TMZ is critical to prolong the survival time of GBM patients. Here, we suggest that both XLF and 53BP1 have the potential to be targeted. HSU2018 may provide a treatment option for patients that are less sensitive to TMZ. In addition, standard GBM treatments include radiation that generates DNA damages. These DNA damages majorly rely on NHEJ for repair. Therefore, elevated NHEJ efficiency could also impair radiation therapy. As an inhibitor of NHEJ key factor, we hypothesize that HSU2018 can also sensitize GBM cells to radiation.

Abbreviations

GBM, glioblastoma; TMZ, temozolomide; NHEJ, non-homologous end joining; HR, homologous recombination; DSB, DNA double-strand break; DNA-PKcs, DNA-dependent protein kinase catalytic subunit; XRCC4, X-ray repair cross-complementing 4; XLF, XRCC4-like factor protein.

Availability Of Data And Materials

All data generated or analyzed during this study are included in this published article.

Funding

Promotive Research Fund for Young and Middle-Aged Scientists of Shandong Province (BS10YY026 to Lingyi Chi), Independent Innovation Foundation of Shandong University (IIFSDU 2012TS144 and 2015TS017 to Lingyi Chi), Shandong Province Natural Science Foundation (ZR2017MH129 to Jie Chai) and Shandong Province key research and development plan (GG201710070085 to Jie Chai).

Disclosure

The authors declare that they have no competing interests.

References

1. Inskip PD, Linet MS, Heineman EF. Etiology of brain tumors in adults. *Epidemiol Rev*. 1995;17(2):382–414. doi:10.1093/oxfordjournals.epirev.a036200
2. Beroukhim R, Getz G, Nghiemphu L, et al. Assessing the significance of chromosomal aberrations in cancer: methodology and application to glioma. *Proc Natl Acad Sci U S A*. 2007;104(50):20007–20012. doi:10.1073/pnas.0710052104
3. Patel AP, Tirosh I, Trombetta JJ, et al. Single-cell RNA-seq highlights intratumoral heterogeneity in primary glioblastoma. *Science*. 2014;344(6190):1396–1401. doi:10.1126/science.1254257
4. Stupp R, Hegi ME, Mason WP, et al. Effects of radiotherapy with concomitant and adjuvant temozolomide versus radiotherapy alone on survival in glioblastoma in a randomised phase III study: 5-year analysis of the EORTC-NCIC trial. *Lancet Oncol*. 2009;10(5):459–466. doi:10.1016/S1470-2045(09)70025-7
5. Nanegrungsunk D, Onchan W, Chattipakorn N, Chattipakorn SC. Current evidence of temozolomide and bevacizumab in treatment of gliomas. *Neurol Res*. 2015;37(2):167–183. doi:10.1179/1743132814Y.0000000423
6. Chamberlain MC. Temozolomide: therapeutic limitations in the treatment of adult high-grade gliomas. *Expert Rev Neurother*. 2010;10(10):1537–1544. doi:10.1586/ern.10.32
7. Patil SA, Hosni-Ahmed A, Jones TS, Patil R, Pfeffer LM, Miller DD. Novel approaches to glioma drug design and drug screening. *Expert Opin Drug Discov*. 2013;8(9):1135–1151. doi:10.1517/17460441.2013.807248
8. Kanzawa T, Bedwell J, Kondo Y, Kondo S, Germano IM. Inhibition of DNA repair for sensitizing resistant glioma cells to temozolomide. *J Neurosurg*. 2003;99(6):1047–1052. doi:10.3171/jns.2003.99.6.1047
9. Atkins RJ, Ng W, Stylli SS, Hovens CM, Kaye AH. Repair mechanisms help glioblastoma resist treatment. *J Clin Neurosci*. 2015;22(1):14–20. doi:10.1016/j.jocn.2014.09.003
10. Lieber MR. The mechanism of double-strand DNA break repair by the nonhomologous DNA end-joining pathway. *Annu Rev Biochem*. 2010;79:181–211. doi:10.1146/annurev.biochem.052308.093131
11. Chang HHY, Pannunzio NR, Adachi N, Lieber MR. Non-homologous DNA end joining and alternative pathways to double-strand break repair. *Nat Rev Mol Cell Biol*. 2017;18(8):495–506. doi:10.1038/nrm.2017.48
12. Burma S, Chen BP, Chen DJ. Role of non-homologous end joining (NHEJ) in maintaining genomic integrity. *DNA Repair (Amst)*. 2006;5(9–10):1042–1048. doi:10.1016/j.dnarep.2006.05.026
13. Jasin M, Rothstein R. Repair of strand breaks by homologous recombination. *Cold Spring Harb Perspect Biol*. 2013;5(11):a012740. doi:10.1101/cshperspect.a012740
14. Rothkamm K, Kruger I, Thompson LH, Lobrich M. Pathways of DNA double-strand break repair during the mammalian cell cycle. *Mol Cell Biol*. 2003;23(16):5706–5715. doi:10.1128/MCB.23.16.5706-5715.2003
15. Hinz JM, Yamada NA, Salazar EP, Tebbs RS, Thompson LH. Influence of double-strand-break repair pathways on radiosensitivity throughout the cell cycle in CHO cells. *DNA Repair (Amst)*. 2005;4(7):782–792. doi:10.1016/j.dnarep.2005.03.005
16. Jasin M. Genetic manipulation of genomes with rare-cutting endonucleases. *Trends Genet*. 1996;12(6):224–228. doi:10.1016/0168-9525(96)10019-6
17. Interthal H, Chen HJ, Kehl-Fie TE, Zotzmann J, Leppard JB, Champoux JJ. SCAN1 mutant Tdp1 accumulates the enzyme–DNA intermediate and causes camptothecin hypersensitivity. *Embo J*. 2005;24(12):2224–2233. doi:10.1038/sj.emboj.7600694
18. Li J, Summerlin M, Nitiss KC, Nitiss JL, Hanakahi LA. TDP1 is required for efficient non-homologous end joining in human cells. *DNA Repair (Amst)*. 2017;60:40–49. doi:10.1016/j.dnarep.2017.10.003
19. Heo J, Li J, Summerlin M, et al. TDP1 promotes assembly of non-homologous end joining protein complexes on DNA. *DNA Repair (Amst)*. 2015;30:28–37. doi:10.1016/j.dnarep.2015.03.003
20. Yannone SM, Khan IS, Zhou RZ, Zhou T, Valerie K, Povirk LF. Coordinate 5′ and 3′ endonucleolytic trimming of terminally blocked blunt DNA double-strand break ends by Artemis nuclease and DNA-dependent protein kinase. *Nucleic Acids Res*. 2008;36(10):3354–3365. doi:10.1093/nar/gkn205
21. Mahaney BL, Hammel M, Meek K, Tainer JA, Lees-Miller SP. XRCC4 and XLF form long helical protein filaments suitable for DNA end protection and alignment to facilitate DNA double strand break repair. *Biochem Cell Biol*. 2013;91(1):31–41. doi:10.1139/bcb-2012-0058
22. Meng Y, Chen CW, Yung MMH, et al. DUOXA1-mediated ROS production promotes cisplatin resistance by activating ATR-Chk1 pathway in ovarian cancer. *Cancer Lett*. 2018;428:104–116. doi:10.1016/j.canlet.2018.04.029
23. Chen CW, Li Y, Hu S, et al. DHS (trans-4,4′-dihydroxystilbene) suppresses DNA replication and tumor growth by inhibiting RRM2 (ribonucleotide reductase regulatory subunit M2). *Oncogene*. 2018.
24. Sun J, Guo Y, Fu X, et al. Dendrobium candidum inhibits MCF-7 cells proliferation by inducing cell cycle arrest at G2/M phase and regulating key biomarkers. *Onco Targets Ther*. 2016;9:21–30. doi:10.2147/OTT.S93305
25. Seluanov A, Mao Z, Gorbunova V. Analysis of DNA double-strand break (DSB) repair in mammalian cells. *J Vis Exp*. 2010;(43):2002.
26. Guo Y, Fu X, Jin Y, et al. Histone demethylase LSD1-mediated repression of GATA-2 is critical for erythroid differentiation. *Drug Des Devel Ther*. 2015;9:3153–3162. doi:10.2147/DDDT.S81911
27. Chabner BA, Roberts TG Jr. Timeline: chemotherapy and the war on cancer. *Nat Rev Cancer*. 2005;5(1):65–72. doi:10.1038/nrc1529
28. Liu X, Li P, Hirayama R, et al. Genistein sensitizes glioblastoma cells to carbon ions via inhibiting DNA-PKcs phosphorylation and subsequently repressing NHEJ and delaying HR repair pathways. *Radiother Oncol*. 2018;129(1):84–94. doi:10.1016/j.radonc.2018.04.005
29. Gil Del Alcazar CR, Todorova PK, Habib AA, Mukherjee B, Burma S. Augmented HR repair mediates acquired temozolomide resistance in glioblastoma. *Mol Cancer Res*. 2016;14(10):928–940. doi:10.1158/1541-7786.MCR-16-0125
30. Daley JM, Laan RL, Suresh A, Wilson TE. DNA joint dependence of pol X family polymerase action in nonhomologous end joining. *J Biol Chem*. 2005;280(32):29030–29037. doi:10.1074/jbc.M505277200
31. Dimitrova N, Chen YC, Spector DL, de Lange T. 53BP1 promotes non-homologous end joining of telomeres by increasing chromatin mobility. *Nature*. 2008;456(7221):524–528. doi:10.1038/nature07433
32. Mazzarelli P, Parrella P, Seripa D, et al. DNA end binding activity and Ku70/80 heterodimer expression in human colorectal tumor. *World J Gastroenterol*. 2005;11(42):6694–6700. doi:10.3748/wjg.v11.i42.6694
33. Costantini S, Woodbine L, Andreoli L, Jeggo PA, Vindigni A. Interaction of the Ku heterodimer with the DNA ligase IV/Xrcc4 complex and its regulation by DNA-PK. *DNA Repair (Amst)*. 2007;6(6):712–722. doi:10.1016/j.dnarep.2006.12.007
34. Nick McElhinny SA, Snowden CM, McCarville J, Ramsden DA. Ku recruits the XRCC4-ligase IV complex to DNA ends. *Mol Cell Biol*. 2000;20(9):2996–3003. doi:10.1128/MCB.20.9.2996-3003.2000
35. Uematsu N, Weterings E, Yano K, et al. Autophosphorylation of DNA-PKCS regulates its dynamics at DNA double-strand breaks. *J Cell Biol*. 2007;177(2):219–229. doi:10.1083/jcb.200608077
36. Hammel M, Yu Y, Fang S, Lees-Miller SP, Tainer JA. XLF regulates filament architecture of the XRCC4.ligase IV complex. *Structure*. 2010;18(11):1431–1442. doi:10.1016/j.str.2010.09.009
37. Ahnesorg P, Smith P, Jackson SP. XLF interacts with the XRCC4-DNA ligase IV complex to promote DNA nonhomologous end-joining. *Cell*. 2006;124(2):301–313. doi:10.1016/j.cell.2005.12.031

38. Buck D, Moshous D, de Chasseval R, et al. Severe combined immunodeficiency and microcephaly in siblings with hypomorphic mutations in DNA ligase IV. *Eur J Immunol*. 2006;36(1):224–235. doi:10.1002/eji.200535401

39. Riballo E, Woodbine L, Stiff T, Walker SA, Goodarzi AA, Jeggo PA. XLF-Cernunnos promotes DNA ligase IV-XRCC4 re-adenylation following ligation. *Nucleic Acids Res*. 2009;37(2):482–492. doi:10.1093/nar/gkn957